Matrix-Isolation in Cryogenic Water-Ices: Facile Generation, Storage, and Optical Spectroscopy of Aromatic Radical Cations§

Murthy S. Gudipati*,†

Institute for Physical Sciences and Technology, University of Maryland, College Park, Maryland 20742 and NASA Ames Research Center, MS 245-6, Moffett Field, California 94035-1000

Received: October 17, 2003; In Final Form: February 27, 2004

Radical cations of naphthalene and 4-methylpyrene have been generated for the first time in high conversion efficiencies in cryogenic water-ices at 15 K through vacuum ultraviolet photolysis. With these radical cations as probes it is shown that cryogenic water-ices at temperatures below 50 K are of good optical quality and inert matrices to isolate and study the electronic spectroscopic properties of neutral and ionic species in the wavelength region 250−900 nm. The spectral energies of guest-species in the cryogenic water-ices are closely comparable with those observed using rare-gas matrices, indicating similar host−guest interactions in rare-gas matrices and water-ices below 50 K. The radical cations are converted to the corresponding alcohols at temperatures higher than 50 K due to reactions between the host and ionized guest species. Thus, cryogenic water-ices are inert matrices that resemble and complement the rare-gas matrices in many aspects. Efficient ionization of organic molecules, such as PAHs studied here, in water-rich ices indicates that ionization-mediated processes play an important role in the evolution of cosmic ices that are exposed to ionizing radiation.

Introduction

Matrix-isolation, a short form for isolation and stabilization of charged and neutral atoms and molecules in low-temperature solids, is a technique that has been extensively used[1,2] since its introduction by Pimentel and co-workers[3] in the early nineteen-fifties. In the earlier days, rare-gas solids were thought to be ideal materials for matrix-isolation due to their very inert nature to undergo chemical reactions or interactions with the guest species at cryogenic temperatures.[4] However, recent studies show that the rare-gas (Rg) matrices are no longer inert-gas matrices and that several reactions/interactions with the guest-species result in the formation of ground-state Rg molecules with covalent or ionic bonds.[5,6] Thus, there is a partial reversal of role played by the Rg matrices during the past few decades from inert to sometimes reactive. Other relatively inert low-temperature solids such as H_2,[7] N_2,[8] CH_4,[9] and SF_6[10] have also been often used for matrix-isolation studies,[4] among which *para*-hydrogen[11,12] has gained considerable interest in recent times due to its unique properties as a quantum solid. On the other hand, oxygen-containing low-temperature solids such as O_2,[13] and CO_2[14] are less known as matrix materials due to their high propensity toward reactions/interactions with the guest species. Similarly, one does not often find in the literature explicit mention of water-ices as potential matrices. Possibly, low-temperature H_2O-ice is also assumed to be a reactive medium for the isolation and stabilization of reactive intermediates and/or stable molecules. It will be shown in this article that the role-reversal for the Rg matrices—inert to reactive—also applies to the water matrices, namely—reactive to inert—making water-ices potential medium for matrix-isolation studies.

Cryogenic water-rich ices, as well as the CO and CO_2 ices, are ubiquitous in the interstellar medium[15] and in our Solar System,[16−18] in such places as planets, moons, satellites, and comets; especially the continued finding of water-ices on Mars[19] has attracted considerable attention in recent years. Recent laboratory studies show that photolysis of these water-rich cosmic ice analogues containing CH_3OH, NH_3, CO, and CO_2 with vacuum ultraviolet (VUV) light and subsequent warm-up leads to the formation of biologically important molecules such as amino acids[20,21] and fatty acids that form vesicles.[22] Water-rich ices, thus, could have played an important role in the prebiotic processes toward the origins of life on Earth and elsewhere.[23] On the other hand, there has been a tremendous advancement in the spectroscopic studies of these astronomical icy objects using ground-based and satellite-mounted telescopes, which has led to the accumulation of a large body of information in recent years. To understand the physics and chemistry of these icy bodies, it is extremely important to undertake laboratory experiments that simulate the astrophysical conditions as closely as possible, such as photon and ion bombardment of ices.[24,25] In Earth's atmosphere, ices in the form of aerosols[26] and polar ices[27] also play an important role. The transport of anthropogenic pollutants through aerosols to the polar ices and subsequent chemistry of these ices imbedded with the foreign species is also an important aspect of Earth's environmental changes.[28] Thus, there exists an urgent need to understand the fundamental processes, mechanisms of reactions that are triggered by photons, ions, and electrons at various temperatures in the water-rich ices. Hence, spectroscopy and photochemistry of water-ices containing various impurities at various temperatures and pressures is an emerging aspect of physics and chemistry of ices. In this context, *matrix-isolation* using H_2O-ices is an apt technique whose applications range from astrophysics to atmospheric sciences as mentioned above. A detailed discussion of the astrophysical implications of molecular ions in water-rich ices can be found in our recent publication.[29]

Past studies on low-temperature water-ices (from here on, *ices*) are mostly focused on the infrared spectroscopy.[30−33]

* E-mail: gudipati@glue.umd.edu.
† Also associated with Institut für Physikalische Chemie, Universität zu Köln, Germany.
§ Dedicated to Professor Josef Michl on the occasion of his 65th birthday.

10.1021/jp037152b CCC: $27.50
Published on Web 04/28/2004

However, in the IR spectral region, due to strong absorption by ice itself around 3600 (υ_1 & υ_3), 1600 (υ_2), 700 (L_2) and 400 (L_1) cm^{-1},[34] the transparent windows are restricted, leaving access to only certain types of species to be studied in water-ices. On the other hand, in the optical region, ices are transparent above 160 nm.[35] Outstanding work has been published by Quickenden and collaborators/co-workers on the optical spectroscopy of irradiated and ion-bombarded pure water-ices at low-temperatures.[18,36−40] As will be shown here, cryogenic ices are excellent and diverse matrix-material to undertake spectroscopic studies in the UV−visible (VIS)−near-infrared (NIR) regions ranging between 250 and 900 nm and some parts of the mid-infrared region. Cryogenic ices, when used in conjunction with the rare-gas matrices, can lead to more detailed information about the guest-species due to the large dipole moment of water molecules, inducing changes in the spectral properties of certain species that can interact with water molecules involving hydrogen bonding or dipole−dipole interactions at a local structural level, compared to the apolar species. One can expect spectral shifts proportional to the dipole moment of the solute molecules in ice matrices, whereas such an effect would be minimal in Rg matrices. Electronic spectroscopy of polycyclic aromatic hydrocarbons (PAHs) and their radical cations in cryogenic ices will be presented and discussed here. Further advantages of using cryogenic water-ices in conjunction with the rare-gas matrices will be discussed.

Experimental Section

Naphthalene (NAP) and 4-methylpyrene (4MP) were purchased from Aldrich (99.99% purity) and were used without further purification. Water was purified by three freeze−pump−thaw cycles under vacuum before vacuum transfer into a glass bulb prior to deposition. H_2O/PAH ices were prepared in a high-vacuum, cryogenic sample chamber by co-deposition onto a MgF_2 window at 15 K. For the preparation of the H_2O/NAP matrices (dilution > 200:1), premixed water and NAP gas was deposited under vacuum directly onto the 15 K MgF_2 substrate. For the H_2O/4MP matrices, water vapor was passed over 4MP at room-temperature. resulting in a dilution of H_2O/4MP (∼500:1).[41] Samples were typically deposited at a flow rate of 0.02 mmol/h for 2 to 4 h. At this slow deposition rate, the optical quality of the ices was excellent. After deposition, absorption and emission spectra of the ice were measured. The sample was then VUV-irradiated using a microwave-powered, flowing hydrogen-discharge lamp which produces radiation at Ly_α (121.6 nm) and a roughly 20-nm wide molecular transition centered at 160 nm.

All the experiments were carried out at the NASA Ames Astrochemistry Laboratory. Optical spectra of PAH/H_2O ices were recorded at different doses of VUV radiation. The optical setup is shown in Figure 1. For absorption studies, light from a 150 W Xe arc-lamp (Osram/Oriel) was diverted through a prism, collimated through a lens and finally passed through a 3.0 OD neutral density filter, and an aperture, onto the matrices. The transmitted light was then collimated and focused on the entrance slits of a 0.25 m monochromator (Oriel MS 257) equipped with a CCD camera (Oriel-InstaspecIV) to record the single-beam spectra.

Initial experimental trials showed that the optical quality of the ices was very sensitive to the rate of deposition, VUV irradiation, and thermal history. Unlike rare gases, water leads to the formation of highly scattering films (matrices) unless care is taken to deposit matrices slowly. Under the present conditions, approximately 0.02 mmol h^{-1} deposition rate resulted in ∼10 μm thick ice films over 4 h of deposition at 15 K, assuming all the water gets deposited on the window. Ice matrices obtained in this way were optically clear. The second problem encountered during the present studies was the long-term changes in the scattering properties of the ices caused by photolysis of not only the imbedded PAH molecules, but also the H_2O host by the VUV-photons of the hydrogen lamp. For this reason, single-beam transmission spectra measured were stored in the computer at each event of photolysis or warm-up at small time intervals. Absorption spectra were computed by taking the immediately previous event single-beam spectrum as the background/reference. Absorption spectra obtained in this way were then baseline-corrected over a large spectral range and added together. This procedure is sensitive enough to record absorbances of the order 10^{-3} on short time scales, as seen in Figure 4. A detailed description of this optical setup is also provided elsewhere.[42]

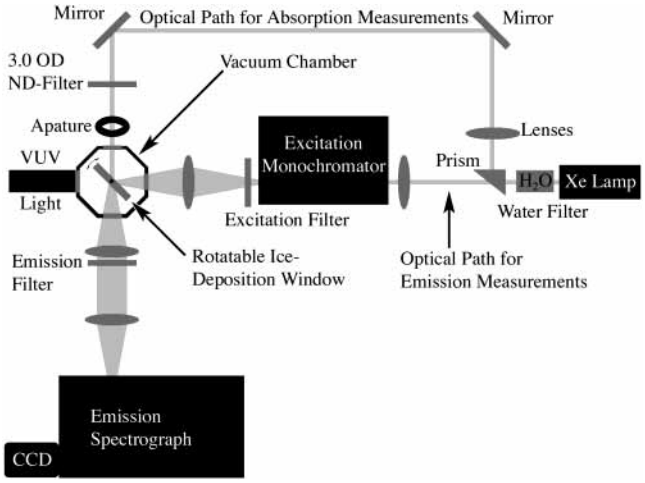

Figure 1. Experimental setup used to measure single-beam electronic absorption and electronic emission spectra of cryogenic water-ices containing PAH and PAH^+ species. By placing the prism next to the water-filter of the Xe-lamp into the beam, the absorption spectra could be measured. For fluorescence spectroscopy, this prism was removed.

The emission spectra were measured by focusing the light from the same Xe arc-lamp onto the entrance slit of a 0.2 m excitation monochromator (Photon Technology International), with which the excitation wavelength could be selected. To avoid light contamination from higher grating-orders, appropriate filters were used at the exit slit of the excitation monochromator before the light was focused onto the matrices. The emission from PAH/H_2O ices induced by this excitation was then collimated and focused onto the entrance slits of the same 0.25 m monochromator used for absorption measurements, and the emission spectra were recorded with the CCD camera, as described above (Figure 1). Though, in principle, both absorption and fluorescence (emission) spectra could have been measured from the sample at any given point of time by changing the positions of the prism shown in Figure 1, due to the fact that the experiments have been carried out to derive quantitative information from weak absorption features, freshly prepared ices were used exclusively either for the absorption or for emission studies.

Results

Figures 2−5 summarize the experiments on NAP/H_2O matrices. Fluorescence of NAP in the ice matrix closely resembles the low-resolution spectrum of NAP in the Ar matrix reported by Najbar and Turek[43] (Figure 2), surprisingly with

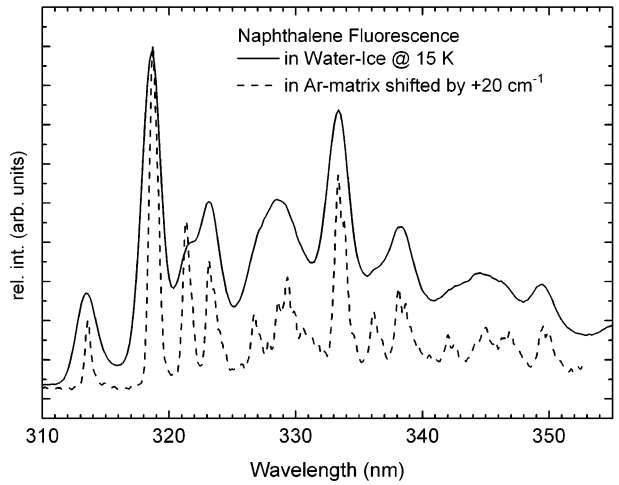

Figure 2. Fluorescence spectrum of naphthalene (NAP) isolated in water-ices at 15 K when excited at 270 nm. Also given in the figure is the spectrum of naphthalene fluorescence in Ar matrix reported in ref 43. Worth noting is the negligible spectral shifts (+20 cm^{-1}).

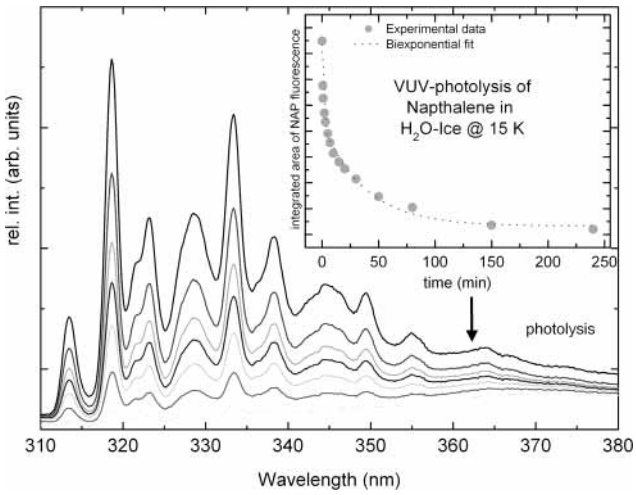

Figure 3. Fluorescence spectra of naphthalene in H_2O ice at 15 K as a function of photoionization with VUV-light (hydrogen flow-discharge lamp). Excitation wavelength is at 270 nm. In the insert, a biexponential decay of naphthalene fluorescence is shown.

almost no spectral shift, namely at 20 cm^{-1}. VUV-photolysis of NAP was monitored by its fluorescence spectrum, as shown in Figure 3. Nearly 85% of the initial NAP fluorescence is depleted during the 150-min irradiation. Integrated fluorescence intensity of NAP is plotted against time, shown as an insert in Figure 3. A biexponential decay gave the best fit to the experimentally observed data, indicating two major NAP photodepletion channels that are independent of each other, one being very fast (half-life 38 s) compared to the other (half-life ~1000 s). The fast depletion channel was not observed in the case of 4MP/H_2O photolysis experiments, where the photodepletion was close to single exponential (vide infra). Concentration-dependent photolysis experiments need to be carried out to resolve the nature of the fast component of the NAP/H_2O photolysis. We note that the only difference between NAP/H_2O and 4MP/H_2O matrices is the concentration of the solute being ~0.5% (NAP) and ~0.2% (4MP). However, it is likely that due to high vapor pressure of NAP, formation of dimers could be significant and the fast channel mentioned above represents that photolysis of dimers. Absorption spectra measured after successive VUV-photolysis steps are shown in Figure 4. The broad absorption centered around 685 nm is due to the NAP^+

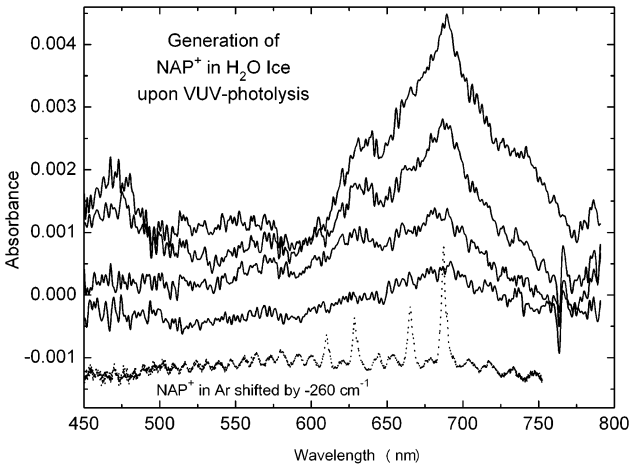

Figure 4. A comparison of the absorption spectra of NAP^+ in ice and in Ar matrices.[44] In addition to the broad-nature of the absorption of the NAP^+ in H_2O, the bands are shifted by 255 cm^{-1} (13 nm) compared to the spectra in Ar matrix. Spectra in ice matrices were measured after 2, 5, 13, and 28 min of VUV-photolysis.

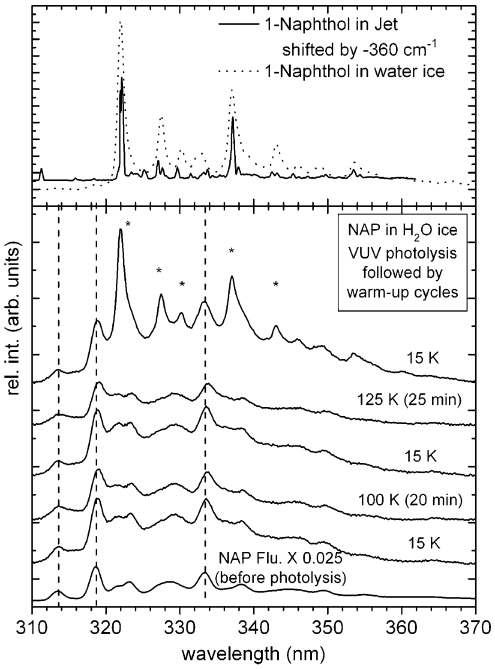

Figure 5. Fluorescence from 1-naphthol formed during the warm-up of NAP^+/H_2O ices. Due to the excited-state proton transfer (ESPT) between 1-naphthol and H_2O at higher than 65 K, fluorescence is detected only at lower temperatures, in accordance with other observations on naphthols in ices.[66] A proton order−disorder phase transition (Ih-XI) occurs in crystalline ices at 72 K. Observation of 1-naphthol fluorescence only after warming the ices to 125 K indicates that there is a reaction-barrier between NAP^+ and the VUV-photolyzed H_2O surrounding in order to form 1-naphthol.

(naphthalene radical cation), whose absorption maximum is red-shifted in H_2O by ~260 cm^{-1} from the maximum measured at 673 nm in the Ar matrix.[44] The unusually broad nature of the absorption can either be due to the shortening of the excited-state lifetime or due to inhomogeneous broadening or both. Further experiments are underway to get concentration-dependent absorption spectra of NAP^+.

During the fluorescence measurements on NAP/H_2O matrices, after VUV-photolysis of over 85%, ice matrices were warmed in order to monitor the changes in the spectra (the product formation from the NAP^+). To rule out the role of artifacts due to physical changes in the ices at higher temperatures, after

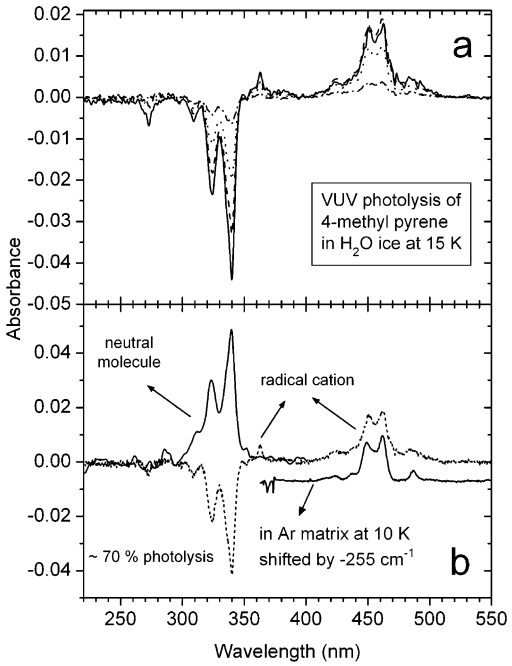

Figure 6. (a) Depletion of 4-methylpyrene (4MP) absorption (∼340 nm) and increase in the $4MP^+$ absorption (∼450 nm) upon VUV-photolysis of $4MP/H_2O$ ice at 15 K using a hydrogen flow-discharge lamp. (b) Contrary to the ∼15% photoionization of PAH molecules in rare-gas matrices,[47] in water-ices close to quantitative (70% of 4MP) photolysis of the neutral species to the corresponding radical cations is achieved. The spectrum of $4MP^+$ in H_2O is shifted by -255 cm^{-1} (toward longer wavelength) compared to the spectrum measured in Ar matrix.[71]

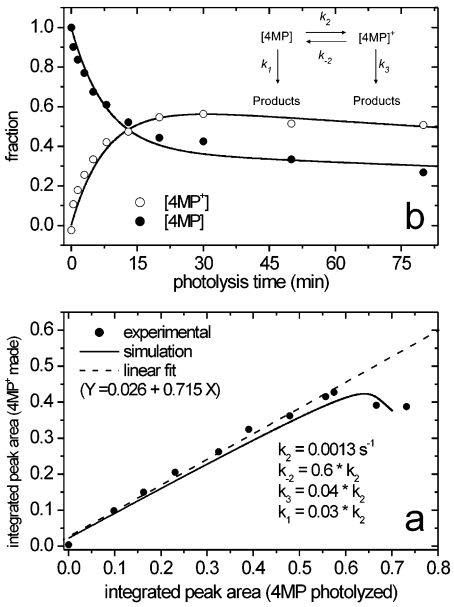

Figure 7. Kinetics of VUV irradiation of the $H_2O/4MP$ (>500:1) ice at 15 K. Solid and open circles are experimental data, whereas the solid and dashed lines are from numerical fits (see text). Absorption bands were integrated and normalized to the integrated absorbance of 4MP before photolysis. *Top*: The fractions of 4MP lost and $4MP^+$ produced are plotted against photolysis time. *Bottom*: Normalized integrated absorbance of 4MP plotted against $4MP^+$ as a function of photolysis sequence. A linear fit from 0 to 2000 s (dashed line) yields the slope of 0.715, which relates the oscillator strengths of the neutral with the cation for the corresponding transitions.

keeping the ices at each temperature for about 20 min and measuring the fluorescence spectra, matrices were cooled to 15 K and fluorescence was measured again. Figure 5 summarizes these results, and in addition shows that no significant changes in the intensity of the neutral NAP fluorescence, and hence no geminate recombination of NAP^+ with electron (marked by dashed vertical lines), reveal new fluorescence bands (marked by asterisks) that are from the oxidation product 1-naphthol, due to the reaction of NAP^+ with VUV-photolyzed H_2O species in its surroundings. The fluorescence spectrum of 1-naphthol in ice matrices is red-shifted by 345 cm^{-1} from the spectrum obtained in supersonic jet.[45] Due to excited-state proton transfer (ESPT) between 1-naphthol and the host H_2O at temperatures >65 K, fluorescence of 1-naphthol is completely suppressed at higher temperatures. This is the reason the fluorescence marked by asterisks is not observed at 125 K, at which temperature 1-naphthol is produced from NAP^+, but only after cooling to 15 K. A phase transition, known as Ih−XI proton ordering transition, occurs[46] at 72 K that suppresses ESPT between the host and guest molecules at lower temperatures, leading to normal fluorescence from the guest molecules, in this case 1-naphthol.

Figures 6 to 8 show the similar experimental results with $4MP/H_2O$ ice matrices. Due to the fact that both neutral and radical cation have significant absorption cross-sections (oscillator strengths) in the same spectral region, it was possible to quantitatively compare the depletion of the neutral 4MP and the generation of $4MP^+$ upon VUV-photolysis, as shown in Figure 6. The spectroscopic information derived from experiments shown in Figure 6 is used to obtain the photolysis rates and product ratios, which are summarized in Figure 7. The disappearance of the radical cation $4MP^+$ upon warming the ices, by monitoring its absorption at 460 nm, is shown in Figure 8. The temperature-dependent semiquantitative plots of the disappearance of $4MP^+$ when $4MP/H_2O$ matrices were studied, and production of 1-naphthol when NAP/H_2O matrices were studied, are shown in Figure 9.

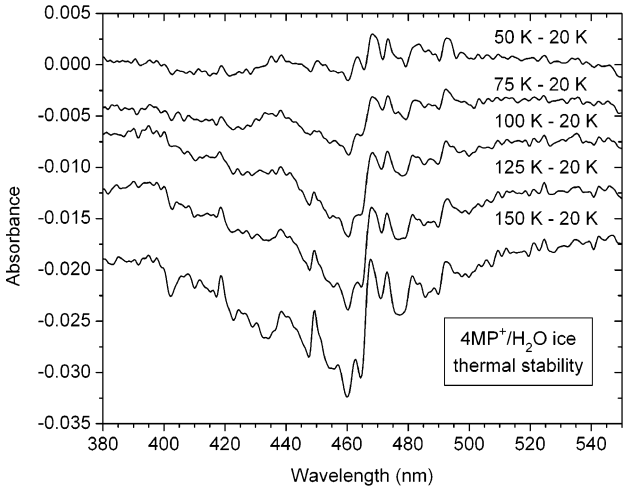

Figure 8. Thermal behavior of $4MP^+$ in H_2O-ices. The spectra shown here were obtained by taking the single-beam spectrum after the VUV-photolysis as the reference. Hence, the negative absorbances indicate depletion of $4MP^+$. Losses of the radical cations below 50 K are negligible. Between 50 and 150 K there is a steady depletion of the absorption due to the radical cation, amounting to complete depletion at 150 K.

Discussion

Generation and Stabilization of PAH^+ in Ices. The most surprising result is the near-to-quantitative photoionization of PAH molecules into their radical cations. In Rg matrices, only

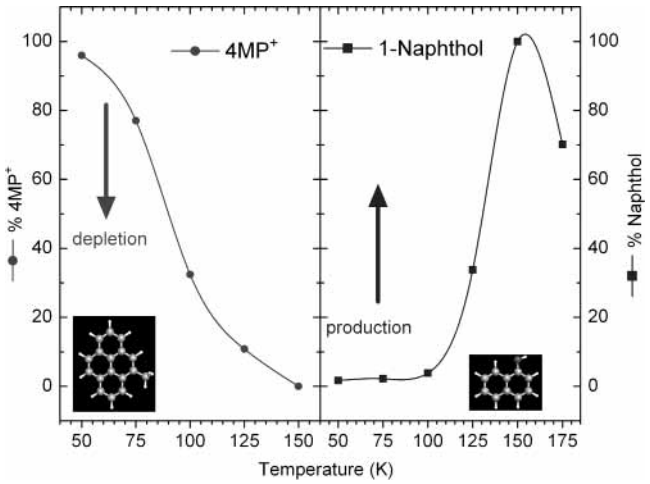

Figure 9. *Left*: Thermal depletion of $4MP^+$ normalized absorption intensity between 50 and 150 K from VUV-photolyzed $4MP/H_2O$ matrices. *Right*: Production of 1-naphthol (monitored by its fluorescence) from NAP^+ in VUV-photolyzed NAP/H_2O matrices. By assuming similar reactivities between $4MP^+$ and NAP^+ in ice-matrices, formation of intermediates at temperatures below 125 K, leading to the formation of stable products above this temperature, can be inferred.

about 15% of the neutral molecules are converted into radical cations,[47] (mostly due to the impurities or electron scavengers such as CCl_4 doped in the Rg matrices[48]), whereas in the ice matrices 4MP is photolyzed by 70% and NAP by 85%. From the experiments on 4MP it was possible to follow quantitatively the depletion of neutral and simultaneous generation of radical cations upon VUV-photolysis, as shown in Figure 6. These data were then used to obtain reaction rates and product channels, summarized in Figure 7. When the integrated band intensities (after converting wavelength to wavenumbers) of depleted 4MP and produced $4MP^+$ were plotted against each other, as given in the bottom part of Figure 7, a linear fit could be drawn up to a point of 55% depletion of 4MP. This fit has a slope of 0.715, which number relates the oscillator strengths of the corresponding electronic transitions in the neutral and cation. Oscillator strength of the *long-axis* polarized transition $1^1B_{3u} \leftarrow 1^1A_g$ at 322 nm in neutral pyrene, the parent PAH of 4MP, is known with a greater accuracy to be ~0.33.[49,50] On the other hand, there are inconsistencies in the oscillator strength of the *long-axis* polarized transition $2^2A_u \leftarrow 1^2B_{3g}$ in the pyrene radical cation.[51−53] By assuming that each photolyzed neutral resulted in a radical cation, i.e., no side reactions, oscillator strength for the $4MP^+$ can be estimated to be 0.24, which is in excellent agreement with the most recent time-dependent density functional calculations at 0.219.[54] A second analysis has been carried out as follows. From the integrated intensities of 4MP and $4MP^+$ absorption bands shown in Figure 6, the fraction of 4MP photolyzed and the fraction of $4MP^+$ generated were calculated relative to the integrated absorption intensity of 4MP before photolysis. The fraction of $4MP^+$ generated was obtained at a given time by first normalizing with the 4MP absorption intensity before photolysis and then dividing by the slope of 0.715 mentioned above (Figure 7a). These values are plotted against the time of photolysis in Figure 7b as filled and open circles for 4MP and $4MP^+$, respectively. Assuming the reaction scheme shown as an insert in Figure 7b, all the data points were simultaneously fit using four independent rate constants—namely, k_2, the rate of ionization; k_{-2}, the reverse ion electron recombination rate; k_1, rate of formation of other products form the neutral; and k_3, rate of formation of other products from the cation. The best fit, shown as solid line curves in both Figure 7a and 7b, resulted in values, also shown in Figure 7a. This analysis clearly demonstrates that the photoionization of 4MP to $4MP^+$ (k_2) is the dominating process, followed by the reverse electron−ion recombination (k_{-2}) at 60% of k_2. The other two processes, product formation from neutral or cation, are approximately 1 order of magnitude slower. Most likely, the electron−ion recombination (k_{-2}) is barrier-less, but 40% of the photoionization results in electron ejection from the parent ice-cage, or electron attachment to $OH/H_2O/O$, or both.

The near-to-quantitative ionization of PAH to PAH^+ in water-ice matrices still needs explanation. From the above analysis we can conclude that ionization is facilitated by solvating both ions and electrons by ice matrix to prevent reverse electron−ion recombination to a great extent. This means that either electrons are stabilized in ice-cages (solvated) or react with the water host, as implied above. Such solvation/hydration of excess electrons by water and water-ices is well established in recent literature.[18,37,55] We note that in Rg matrices, when no electron acceptor is added, the conversions under similar dilutions are less than 15%.[47] This again implies that the cage-exit of electrons is an inefficient process in Rg matrices and the major process is the electron−ion recombination. In ice matrices, water itself acts as the electron acceptor/stabilizer, i.e., an electron-sponge. Under the present experimental conditions, the dilutions were of the order of 0.2−0.5% and charge separation in these ices is expected to be around the same percentage. Further studies are underway to investigate the fate of electrons in PAH-doped water-ice matrices upon VUV-photolysis at various PAH concentrations.

On the basis of our initial results,[29] time-dependent density functional (TDDFT) computations were carried out by Woon and Park[56] to address some of the unusual experimental observations. Their theoretical results are in full agreement with the experimental results presented here. These authors found that the ionization energy of PAHs is lowered by about 1.5 to 2 eV in ices. Further, electron affinity of OH increases from 1.75 eV in the gas-phase to 5.06 eV in ices. Thus, they proposed that the facile ionization of PAHs is due to lowering IP and trapping of electrons by OH radicals. These authors have also found that an ice matrix induces only minor spectral shifts in both PAH and PAH ion spectra, in accordance with our experimental study. Thus, the experimental results presented here have been strongly corroborated by theoretical computations as well.

Cryogenic Ice as New Matrices. The spectroscopic data presented in Figures 2 to 9 strongly support the case for cryogenic water-ice to be the new matrix medium for optical spectroscopy of neutral as well as reactive species such as radical cations. As mentioned in the Introduction, because of absorption due to strong vibrational transitions in H_2O in the mid-infrared (200−5000 cm^{-1}) and NIR (5000−10000 cm^{-1}) regions, only certain *window-regions* will be available for spectroscopic purposes − a contrast to Rg matrices, which are transparent from far-infrared to VUV regions (~50−95000 cm^{-1}). Ice matrices are completely transparent in the UV−Vis−NIR spectral region (10000−40000 cm^{-1}). Surprisingly, the matrix-shifts between ice and Ar matrices are nominal, of the order of 20−250 cm^{-1} for electronic transitions in the UV−Vis region. A more detailed discussion follows. Another contrast between ice matrices and rare-gas matrices is the temperature range. Whereas Rg matrices are held through van der Waals forces and hence sublime at much lower temperatures,[4] ice matrices are held together through much stronger hydrogen bonding and are stable up to 150 K. These unique properties of ice matrices

could be explored to undertake optical spectroscopy of biomolecules, especially those whose low-temperature behavior needs to be understood. As the biomolecules such as enzymes, proteins, and DNAs exist in a water-rich environment, it would be straightforward to freeze the aqueous solutions appropriately to create ice matrices.

Matrix-Shifts. The matrix-shifts going from Ar matrices to ice matrices are surprisingly small, almost negligible at +20 cm^{-1} for the neutral molecule NAP and around −260 cm^{-1} for the radical cations NAP^+ and $4MP^+$. For 1-naphthol, there was no Ar-matrix spectrum available to compare. However, a comparison with supersonic-jet spectrum indicates a red-shift of 345 cm^{-1} ($S_1 \rightarrow S_0$, 0−0 energy: 31400 cm^{-1} in jet[45] and 31055 cm^{-1} in ice matrices from the present work). Taking a red-shift in Ar matrices to be ∼138 cm^{-1} from the gas-phase for NAP ($S_1 \leftrightarrow S_0$, the sites-averaged 0−0 energy in cm^{-1}: 32035 in He drops;[57] 32018 in jet, 32075 in Ne matrix, 31880 in Ar matrix, 31782 in Kr matrix, and 31665 in Xe matrix,[58] and from this work at 31900 in H_2O), a more polar molecule such as 1-naphthol does not show abnormal spectral shifts compared to PAH radical cations. These results indicate that cryogenic ice matrices at 15 K behave just like Rg matrices even with respect to matrix-interaction on the spectroscopic properties. Though recent Monte Carlo−quantum mechanical methods[59] predict the solvent-shifts in homogeneous liquids to great accuracy, traditionally matrix-shifts (solvent-shifts) are attributed to the dielectric constant (ϵ) of the matrix medium and the dipole moment of the solute molecule in the ground (μ_0) and excited states (μ_j) in a form similar to eq 1 below.[4,60,61]

$$\Delta\tilde{\nu}_j(\mathrm{cm}^{-1}) = 22679\,\frac{d}{\mathrm{MM}}\left[\frac{\epsilon-1}{2\epsilon+1}(\mu_0\cdot\mu_0 - \mu_0\cdot\mu_j) + \frac{n^2-1}{2n^2+1}(\mu_0\cdot\mu_j - \mu_j\cdot\mu_j)\right] \quad (1)$$

We may note that in eq 1 for a given solute molecule, the parameters d, the mass density of the solute (g/cm^3); MM, the molar mass of the solute in amu; μ_0 and μ_j are invariable. In the present case, except for 1-naphthol, the dipole moments of PAHs and their radical cations are negligibly small. On the other hand, 1-naphthol should have behaved far more differently than the other molecules studied here, due to considerable dipole moment both in the ground and first excited singlet states ($\mu S_0 = 1.7$ D and $\mu S_1 = 2.0$ D, from semiempirical calculations using the INDO/S method). However, such abnormal spectral shifts were not observed for 1-naphthol either, indicating that the dielectric constant (ϵ) of cryogenic ice matrix may have a role to play. The ϵ value for water at 298 K is around 90 and the $(\epsilon - 1)/(2\epsilon + 1)$ term in the above equation is close to 0.5. On the other hand, this value is close to 0.15 for Ar matrices ($\epsilon = 1.66$). [62] Thus we expect a factor of 3 red-shift in ice matrices compared to Ar matrices. This should amount to ∼415 cm^{-1} red-shift (∼3 nm) in the case of NAP fluorescence from the gas-phase values, which is not the case here. Recent theoretical work by Rick and Haymet[63] on the static dielectric constants of water-ices at various temperatures suggests a dramatic drop in the dielectric constant of water-ices below 50 K due to proton ordering (proton order−disorder Ih−XI transition that is also responsible for ESPT at > 70 K). At 10 K, these authors compute the static dielectric constant of water-ice dramatically dropping 2 orders of magnitude to close to 1, with some uncertainty based on the method used. If indeed the dielectric constant of ice matrices at 15 K is comparable with that of Rg matrices, around 1−2, then one can understand why the matrix-shifts in ice matrices are not abnormal compared to Rg matrices. Experimental measurements on the dielectric constant of ice matrices between 10 and 70 K need to be carried out.

Thermally Induced Reactions. Unlike the Rg matrices, which are mostly face-centered cubic (FCC) crystals,[4] water-ices are more complex solids, spanning amorphous to several crystalline phases. Briefly, when deposited at 15 K, water-ices are amorphous and upon subsequent annealing to ∼150 K become crystalline (Ih).[64] Crystalline ice is known to be converted to the amorphous phase upon ion or VUV-photon irradiation.[65] This crystalline Ih ice undergoes proton-order phase transition (Ih−XI) at 72 K.[66] As mentioned earlier, ice matrices are stable up to around 150 K under high-vacuum (∼10^{-7} mbar); at higher temperatures the water-ices start subliming, which becomes complete by 185 K.[64] VUV-irradiated amorphous ices show reactivity already at lower temperatures, as shown in Figure 5 for the formation of 1-naphthol from NAP^+. Only after warming up to 125 K was the fluorescence from 1-naphthol detected, indicating a barrier for the reaction between NAP^+ and the surrounding VUV-photolyzed H_2O. However, the absorption spectra of $4MP^+$ indicate that the cation starts disappearing already at 75 K, as shown in Figure 8. It may be noted that products that are formed from $4MP^+$ could not be followed due to the lack of unique emission or absorption features. In Figure 9, the temperature-dependent disappearance of $4MP^+$ from $4MP/H_2O$ experiments and the appearance of 1-naphthol from NAP/H_2O experiments are plotted. Under the assumption that the radical cations $4MP^+$ and NAP^+ show similar reactivity in water-ices, we find that between ∼75 and 125 K, though the PAH^+ disappears significantly (inferred from $4MP^+$), final products are not yet formed (inferred from 1-naphthol), indicating the formation of intermediate complexes that do not resemble either the PAH^+ or the aromatic alcohol. One such possibility for the intermediate is 1-hydro-1-naphthol, due to the addition of a hydroxyl radical or anion at the α position of NAP^+. Theoretical computations on such intermediate formations have been carried out by Ricca and Bauchlicher, Jr.,[67] which are in accordance with the present observations.

Astrophysical and Atmospheric Relevance of Ionization in Ices. Present work on ices was motivated by its relevance to astrophysics and origins of life. Similarly, the ices in the form of aerosols in the troposphere, the stratosphere, and polar ice caps and their chemistry also play an important role in atmospheric processes.

Water-rich ices exist at cryogenic temperatures between 10 and 20 K in dense molecular clouds that form a part of the life-cycle of stars.[15,68] In our Solar System, water-ices at temperatures ranging from 30 to 150 K contribute to the atmospheres of planetary bodies.[16,17] In Earth's atmosphere, water-ices in the form of aerosols transport pollutants and undergo important photochemical reactions.[26,27] Thus, ionization of impurities in ices and subsequent chemistry at various temperatures may contribute significantly toward the ice-chemistry wherever the required energy is available in the form of photons, electrons, or ions (cosmic rays). Laboratory experiments have shown that bombardment with either high-energy photons or protons (model cosmic rays) results in similar chemistry,[24] indicating that the form of the energy deposited into the ices is less important than its ability to electronically excite impurities. Given this, ionization-mediated processes in water-rich ices need to be taken into account to understand the physics and chemistry of Earth's atmospheric aerosols, icy bodies in our Solar System, including comets, as well as ices in interstellar dense molecular clouds. The past and present

laboratory experiments predict that in these environments, electronic processes such as dissociation and ionization followed by thermal reactions among these radicals and ions leads to oxidation products.[25,69,70] These oxidation products span a wide class of important biogenic molecules such as amino acids, fatty acids, alcohols, and ketones. Present work shows that ionization is one of the key steps in water-rich ices in the formation of biogenic molecules and could have contributed to the evolution of life on planet Earth.

Conclusions

Cryogenic water-ices are found to be new matrices for optical spectroscopy, which facilitate photoionization of aromatic molecules. Counterintuitively, at 15 K the radical cations of PAHs are stable for long periods of time. Another surprise is the matrix-shifts of electronic transitions to be comparable to that of rare-gas matrices, especially Ar. This observation is at present anchored on the theoretical work that the static dielectric constant of water-ice drops 2 orders of magnitude to ~1 at cryogenic temperatures (<50 K) due to proton order−disorder transition in the crystalline ice. Why amorphous and crystalline cryogenic ices also behave as if their dielectric constant is close to those of rare-gases needs to be further investigated. Recent TDDFT computations by Woon and Park[56] on PAHs and their radical cations in water-ices render further support to our experimental observations presented here. It may be cautioned that the spectroscopic observations presented here, such as inertness of ice matrices toward the electronic spectra of solute PAH molecules, should not be generalized to all molecules and species. Small diatomics and open-shell species such as OH are known to interact strongly with the ice matrix, changing the electronic properties of OH.[38]

Facile ionization of impurities in water-ices has important implications for astrophysics and atmospheric sciences. The present work opens new insights into the energy deposition and dissipation as well as chemical processes that occur in ices at various equilibrium temperatures. It is important to investigate how strongly the ionization energies of the impurities are altered (lowered) in water-ices at various temperatures by undertaking a wavelength-dependent photolysis study. Theoretical work of Woon and Park[56] predicts lowering of ionization potential up to 2 eV for small PAHs. Finally, ionization, and by implication, ion-mediated processes in water-rich ices, could have played an important role in the evolution of biogenic molecules on early Earth or in comets or elsewhere in the universe.

Acknowledgment. The author is greatly indebted to Dr. Lou Allamandola for excellent discussions, encouragement, and strong support at NASA Ames and to Prof. Marshall Ginter at University of Maryland. The author thanks Drs. Max Bernstein and Jason Dworkin for helpful discussions. Financial support of NASA Ames subcontract to University of Maryland is gratefully acknowledged (Grant No. NCC 12303).

References and Notes

(1) Bondybey, V. E.; Smith, A. M.; Agreiter, J. *Chem. Rev.* **1996**, *96*, 2113.
(2) Apkarian, V. A.; Schwentner, N. *Chem. Rev.* **1999**, *99*, 1481.
(3) Whittle, E.; Downs, D. A.; Pimentel, G. C. *J. Chem. Phys.* **1954**, *22*, 1943.
(4) Mayer, B. *Low-Temperature Spectroscopy*; Elsevier: New York, 1971.
(5) Pettersson, M.; Lundell, J.; Räsänen, M. *Eur. J. Inorg. Chem.* **1999**, 729.
(6) Pettersson, M.; Khriachtchev, L.; Lignell, A.; Räsänen, M.; Bihary, Z.; Gerber, R. B. *J. Chem. Phys.* **2002**, *116*, 2508.
(7) Wang, X. F.; Andrews, L. *J. Phys. Chem. A* **2003**, *107*, 570.
(8) Broquier, M.; Crépin, C.; Cuisset, A.; Dubost, H.; Galaup, J. P.; Roubin, P. *J. Chem. Phys.* **2003**, *118*, 9582.
(9) Legay-Sommaire, N.; Legay, F. *Chem. Phys.* **1996**, *211*, 367.
(10) Mohammed, H. H. *J. Chem. Phys.* **1990**, *93*, 412.
(11) Fajardo, M. E.; Tam, S. *J. Chem. Phys.* **1998**, *108*, 4237.
(12) Tam, S.; Macler, M.; DeRose, M. E.; Fajardo, M. E. *J. Chem. Phys.* **2000**, *113*, 9067.
(13) Hashimoto, S.; Akimoto, H. *J. Phys. Chem.* **1987**, *91*, 1347.
(14) Samuni, U.; Haas, Y.; Fajgar, R.; Pola, J. *J. Mol. Struct.* **1998**, *449*, 177.
(15) Ehrenfreund, P.; Charnley, S. B. *Annu. Rev. Astron. Astrophys.* **2000**, *38*, 427.
(16) Roush, T. L. *J. Geophys. Res.-Planets* **2001**, *106*, 33315.
(17) Cruikshank, D. P.; Brown, R. H.; Calvin, W. M.; Roush, T. L.; Bartholomew, M. J. Ices on the satellites of Jupiter, Saturn, and Uranus. In *Solar System Ices*; Schmitt, B., de Bergh, C., Festou, M., Eds.; Kluwer Academic Publishers: Dordrecht, The Netherlands, 1998; p 576.
(18) Johnson, R. E.; Quickenden, T. I. *J. Geophys. Res.* **1997**, *102*, 10985.
(19) Titus, T. N.; Kieffer, H. H.; Christensen, P. R. *Science* **2003**, *299*, 1048.
(20) Bernstein, M. P.; Dworkin, J. P.; Sandford, S. A.; Cooper, G. W.; Allamandola, L. J. *Nature* **2002**, *416*, 401.
(21) Muñoz Caro, G. M.; Meierhenrich, U. J.; Schutte, W. A.; Barbier, B.; Arcones Segovia, A.; Rosenbauer, H.; Thiemann, W. H.-P.; Brack, A.; Greenberg, J. M. *Nature* **2002**, *416*, 403.
(22) Dworkin, J. P.; Deamer, D. W.; Sandford, S. A.; Allamandola, L. J. *Proc. Natl. Acad. Sci.* **2001**, *98*, 815.
(23) Deamer, D.; Dworkin, J. P.; Sandford, S. A.; Bernstein, M. P.; Allamandola, L. J. *Astrobiology* **2003**, *2*, 371.
(24) Gerakines, P. A.; Moore, M. H.; Hudson, R. L. *J. Geophys. Res.-Planets* **2001**, *106*, 33381.
(25) Hudson, R. L.; Moore, M. H. *Astrophys. J.* **2002**, *568*, 1095.
(26) Prenni, A. J.; Tolbert, M. A. *Acc. Chem. Res.* **2001**, *34*, 545.
(27) Klán, P.; Holoubek, I. *Chemosphere* **2002**, *46*, 1201.
(28) Klánová, J.; Klán, P.; Nosek, J.; Holoubek, I. *Environ. Sci. Technol.* **2003**, *37*, 1568.
(29) Gudipati, M. S.; Allamandola, L. J. *Astrophys. J. Lett.* **2003**, *596*, L195.
(30) Sóley Kristjánsdóttir, S.; Norton, J. R.; Moroz, A.; Sweany, R. L.; Whittenburg, S. L. *Organometallics* **1991**, *10*, 2357.
(31) Strazzulla, G.; Leto, G.; Gomis, O.; SaTorre, M. A. *Icarus* **2003**, *164*, 163.
(32) Moore, M. H.; Ferrante, R. F.; Nuth, J. A., III. *Planet. Space Sci.* **1996**, *44*, 927.
(33) Schutte, W. A.; Allamandola, L. J.; Sandford, S. A. *Icarus* **1993**, *104*, 118.
(34) Zelsmann, H. R. *J. Mol. Struct.* **1995**, *350*, 95.
(35) Chergui, M.; Schwentner, N.; Stepanenko, V. *Chem. Phys.* **1994**, *187*, 153.
(36) Cooper, P. D.; Johnson, R. E.; Quickenden, T. I. *Planet. Space Sci.* **2003**, *51*, 183.
(37) Gillis, H. A.; Quickenden, T. I. *Can. J. Chem.* **2001**, *79*, 80.
(38) Langford, V. S.; McKinley, A. J.; Quickenden, T. I. *Acc. Chem. Res.* **2000**, *33*, 665.
(39) Matich, A. J.; Bakker, M. G.; Lennon, D.; Quickenden, T. I.; Freeman, C. G. *J. Phys. Chem.* **1993**, *97*, 10539.
(40) Quickenden, T. I.; Irvin, J. A.; Sangster, D. F. *J. Chem. Phys.* **1978**, *69*, 4395.
(41) Hudgins, D. M.; Allamandola, L. J. *J. Phys. Chem.* **1995**, *99*, 3033.
(42) Gudipati, M. S.; Dworkin, J. P.; Chillier, X. D. F.; Allamandola, L. J. *Astrophys. J.* **2003**, *583*, 514.
(43) Najbar, J.; Turek, A. M. *Chem. Phys. Lett.* **1980**, *73*, 536.
(44) Salama, F.; Allamandola, L. J. *J. Chem. Phys.* **1991**, *94*, 6964.
(45) Knochenmuss, R.; Muiño, P. L.; Wickleder, C. *J. Phys. Chem.* **1996**, *100*, 11218.
(46) Akiyama, T.; Sakamaki, M.; Abe, K.; Shigenari, T. *J. Phys. Chem. B* **1997**, *101*, 6205.
(47) Hudgins, D. M.; Bauschlicher, C. M., Jr.; Allamandola, L. J.; Fetzer, J. C. *J. Phys. Chem. A* **2000**, *104*, 3655.
(48) Salama, F.; Allamandola, L. J. *J. Chem. Phys.* **1991**, *95*, 6190.
(49) Gudipati, M. S.; Daverkausen, J.; Hohlneicher, G. *Chem. Phys.* **1993**, *173*, 143.
(50) Bito, Y.; Shida, N.; Toru, T. *Chem. Phys. Lett.* **2000**, *328*, 310.
(51) Vala, M.; Szczepanski, J.; Pauzat, F.; Parisel, O.; Talbi, D.; Ellinger, Y. *J. Phys. Chem.* **1994**, *98*, 9187.
(52) Hirata, S.; Lee, T. J.; Head-Gordon, M. *J. Chem. Phys.* **1999**, *111*, 8904.
(53) Negri, F.; Zgierski, M. Z. *J. Chem. Phys.* **1994**, *100*, 1387.
(54) Weisman, J. L.; Lee, T. J.; Salama, F.; Head-Gordon, M. *Astrophys. J.* **2003**, *587*, 256.

(55) Khambampati, P.; Son, D. H.; Kee, T. W.; Barbara, P. F. *J. Phys. Chem. A* **2002**, *106*, 2374.
(56) Woon, D. E.; Park, J.-Y. *Astrophys. J.* **2004**, preprint doi: 10.1086/383345.
(57) Stienkemeier, F.; Vilesov, A. F. *J. Chem. Phys.* **2001**, *115*, 10119.
(58) Crépin, C.; Tramer, A. *Chem. Phys.* **2001**, *272*, 227.
(59) Coutinho, K.; Canuto, S.; Zerner, M. C. *J. Chem. Phys.* **2000**, *112*, 9874.
(60) Klessinger, M.; Michl, J. *Excited States and Photochemistry of Organic Molecules*; VCH: New York, 1995.
(61) Karelson, M. M.; Zerner, M. C. *J. Chem. Phys.* **1992**, *96*, 6949.
(62) Jodl, H. J. In *Chemistry and Physics of Matrix-Isolated Species*; Andrews, L., Moskovits, M., Eds.; North-Holland: Amsterdam, 1989; p 343.
(63) Rick, S. W.; Haymet, A. D. J. *J. Chem. Phys.* **2003**, *118*, 9291.
(64) La Spisa, S.; Waldheim, M.; Lintemoot, J.; Thomas, T.; Naff, J.; Robinson, M. *J. Geophys. Res.* **2001**, *106*, 33351.
(65) Leto, G.; Baratta, G. A. *Astron. Astrophys.* **2003**, *397*, 7.
(66) Ping, Q.; Okazaki, K.; Akiyama, T.; Abe, K.; Shigenari, T. *Solid State Commun.* **1995**, *95*, 177.
(67) Ricca, A.; Bauchlicher, J. C. W. *Chem. Phys. Lett.* **2000**, *328*, 396.
(68) Charnley, S. B.; Rodgers, S. D.; Ehrenfreund, P. *Astron. Astrophys.* **2001**, *378*, 1024.
(69) Bernstein, M. P.; Elsila, J. E.; Dworkin, J. P.; Sandford, S. A.; Allamandola, L. J.; Zare, R. N. *Astrophys. J.* **2002**, *576*, 1115.
(70) Bernstein, M. P.; Sandford, S. A.; Allamandola, L. J.; Gillette, J. S.; Clemett, S. J.; Zare, R. N. *Science* **1999**, *283*, 1135.
(71) Joblin, C.; Salama, F. Personal Communication.